# DNS experiments on the settling of heavy particles in homogeneous turbulence: two-way coupling and Reynolds number effects

**Anne Dejoan**

Modeling and Simulation Group, Centro de Investigaciones de Energéticas Medioambientales y Tecnológicas (CIEMAT) , Avenida Complutense, 22, 28040, Madrid, Spain

E-mail: anne.dejoan@ciemat.es

**Abstract.**

The present study addresses the effects of two-way fluid-particle interaction ("two-way coupling") on the settling of heavy particles in homogeneous turbulence. The modification of turbulence by the particles and the resulting effects on the settling velocity are analyzed by taking into account Reynolds number effects. The turbulent carrier fluid phase is resolved by direct numerical simulation (DNS) and the particle phase by the Lagrangian point-particle approximation. Results are presented for two Taylor microscale Reynolds numbers $R_\lambda = 40$ and 130. While for $R_\lambda = 40$ the Kolmogorov time scale, $t_\eta$, is found almost unaltered by the two-way coupling, it is found significantly decreased for $R_\lambda = 130$. The consequent modification of the particle Stokes number $St = \tau_p/t_\eta$, $\tau_p$ being the particle response time, shows that comparisons between one-way coupling numerical data and two-way coupling numerical or experimental data may be inconsistent. This is particularly relevant for the particle settling in turbulence which has been previously shown to be strongly influenced by the dynamical interaction of the small flow scales with the particles.

## 1. Introduction

The knowledge of the settling of heavy particles in turbulence is relevant to many environmental and engineering problems such as the settling of aerosol particles in the atmosphere or combustion devices.

Direct numerical simulations that only accounted for the effects of the carrier flow on the particles ("one-way coupling" DNS) have shown that the average settling velocity of heavy particles is increased by turbulence (see Wang & Maxey [1], Yang & Lei [2]). The faster settling of the particles is explained by the coupling of two mechanisms (Wang & Maxey [1]): the tendency of inertial particles to accumulate on the peripheries of vortical structures (referred to as "preferential concentration") and the tendency of particles to

move along the downward fluid motion (referred to as "preferential sweeping"). These numerical studies also showed that the maximum increase of the settling velocity is obtained for particles with response time $\tau_p \sim t_\eta$ (Wang & Maxey [1]), $t_\eta$ being the Kolmogorov time scale, and for terminal velocity in the still fluid $v_t \sim 0.5u'$ (Yang & Lei [2]), $u'$ defining the turbulence intensity. Similar qualitative findings were also observed in the experiments of Aliseda *et al.* [3] and of Yang & Shy [4]. Note that the settling velocity of heavy particles in turbulent flow is a quantity very difficult to measure and that these two experiments are the main ones reported for homogeneous turbulence in the literature.

An important open issue, on which both above experiments do not agree one with each other, is the modification of turbulence by the particles ("two-way coupling") and the resulting effects on the settling velocity. On one hand, Aliseda *et al.* [3] showed that the larger is the volume fraction the larger is the increase of the settling velocity. They explained this result by concentration effects and *a-priori* discarded two-way coupling effects because of the low volume fraction considered, $\Phi_v \sim 10^{-5}$. On the contrary, for similar volume fraction, Yang & Shy [4] found a significant increase of the turbulence energy by the particles but obtained an increase of the settling velocity close to the one obtained by one-way coupling simulations. This in turn suggests that two-way coupling may not alter the settling velocity. Nonetheless, the DNS of Bosse *et al.* [5] do show an additional enhancement of the settling velocity by two-way coupling effects. However, their two-way coupling DNS results poorly compare with the experiments. It is noteworthy to mention that the most complete experimental data set provided by Yang & Shy [4] on both the modification of turbulence by the particles and on the settling velocity, corresponds to a Taylor microscale Reynolds number $R_\lambda = 120$, much higher than the one considered by Aliseda *et al.* [3] ($R_\lambda = 75$) and those used in the DNS, limited to low or moderate Reynolds numbers ($R_\lambda = 40 - 75$). Reynolds number effects are thus not excluded from the numerical and experimental observations.

The present study proposes to further investigate the two-way fluid-particle interaction in the settling of heavy particles by also addressing Reynolds number effects. For this, two-way coupling DNS is used to simulate a particle-laden homogeneous turbulence at a low and a high Reynolds numbers, $R_\lambda = 40$ and 130 (both values allow comparisons with previous numerical and experimental data). Stationary but as well decaying homogeneous turbulence are considered to assess how far the use of a forcing scheme in the simulation of the stationary turbulence may influence the results, especially when two-way coupling are accounted for and at low Reynolds numbers, when the separation between the large scales and the small scales of turbulence is not complete.

## 2. Methodology and flow parameters

The homogeneous and isotropic turbulence is described in the Eulerian frame by the incompressible Navier-Stokes equations

$$\frac{\partial u_i}{\partial t} + u_j \frac{\partial u_i}{\partial x_j} = -\frac{1}{\rho}\frac{\partial p}{\partial x_i} + \nu \frac{\partial^2 u_i}{\partial x_j \partial x_j} + f_i - f_i^{(p)} \tag{1}$$

where $x_i (i = 1, 2, 3)$ are the spatial coordinates, $u_i (i = 1, 2, 3)$ the velocity components, $\rho$ the fluid density, $p$ the pressure, $\nu$ the kinematic viscosity and $f_i$ the external energy

**Table 1.** Numerical and flow parameters. Microscale Reynolds number $R_\lambda$, number of computational nodes $N^3$, viscosity $\nu$, box side length $L_{\text{box}}$, integral length scale $L$, large-eddy turn-over time $T$, Kolmogorov length and time scales $\eta$ and $t_\eta$, maximum wavenumber $k_{\max} = \sqrt{2}N/3$, forcing mode $k_p$ and statistical integration time $T_{\text{stat}}$ (forced flow). Values are based on the unladen flow quantities.

| $R_\lambda$ | $N^3$ | $\nu$ | $L/L_{\text{box}}$ | $L/\eta$ | $T/t_\eta$ | $k_{max}\eta$ | $k_p$ | $T_{\text{stat}}/T$ |
|---|---|---|---|---|---|---|---|---|
| 40 | $64^3$ | 0.0178 | 0.211 | 31.56 | 15.85 | 1.32 | 3 | $\sim 50$ |
| 130 | $512^3$ | 0.00059 | 0.114 | 114.24 | 32.96 | 1.61 | 3.5 | $\sim 11$ |

source term to achieve a statistically steady turbulence ($f_i = 0$ for decaying turbulence). The term $-f_i^{(p)}$ represents the net force per unit mass exerted by a number of $n_p$ particles within the integration control fluid volume and is computed from

$$f_i^{(p)} = \frac{1}{m}\sum_{1}^{n_p} f_{p_i} \tag{2}$$

where $m$ is the mass of fluid within the integration control volume and $f_{p_i}$ is the drag force acting on a particle $p$ in the $x_i$-direction.

The particles, with density $\rho_p$ much larger then the fluid density $\rho$, are described in the Lagrangian frame by the equation of motion of Maxey and Riley [6]

$$m_p\frac{dv_i}{dt} = \underbrace{m_p\frac{(u_{x_{p_i}} - v_i)}{\tau_p}}_{f_{p_i}} + (m_p - m)g_i \tag{3}$$

where $v_i (i = 1, 2, 3)$ are the particle velocity components, $u_{x_{p_i}}$ the instantaneous fluid velocity at the particle location $x_{p_i}$ and $m_p$ the particle mass. The response time of the particles, $\tau_p$, is given by $\tau_p = d^2\rho_p/(18\nu\rho)$ with $d$ the particle diameter; the gravitational acceleration $g_i$ is such that $g_1 = g_2 = 0$ and $g_3 = -|g|$ where $|g|$ is defined from $v_t = -\tau_p|g|(1 - \rho/\rho_p)$, $v_t$ being the terminal velocity of the particles in the still fluid.

The Navier-Stokes equations are solved on a cubic fluid box of side length $L_{\text{box}} = 2\pi$, discretized into $N^3$ computational nodes, with periodic boundary conditions. A fully pseudo-spectral algorithm with a de-aliasing truncation technique (referred to as the "2/3 rule") is used with a second-order Runge-Kutta time-stepping for the non-linear terms and an analytic integrating factor for the viscous terms. The forcing is achieved by introducing a power input distributed over a narrow band of wavenumbers $k$ that satisfy $k_p - 1 \leq k \leq k_p + 1$, where $k_p$ defines the peak forcing mode (see Rogallo [7] and Jímenez & Wray [8] for further computational details). The average mean flow integrated over the flow domain is imposed to be zero throughout the two-way coupling simulations. This is done by applying a mean pressure gradient that balances the net weight of the particle phase in the periodic domain. This avoids any further acceleration

**Table 2.** Particle Stokes number $St = \tau_p/t_\eta$ and normalized diameter; all particles have a density ratio $\rho_p/\rho = 5000$. Values are based on the unladen flow quantities.

| $St$ | 0.36 | 1 | 2 |
|---|---|---|---|
| $d/\eta$ | 0.0359 | 0.0597 | 0.0847 |

of the particles in the gravity direction due to a non-zero net volume flux (see Maxey & Patel [9] and Bosse *et al.* [5]).

In a Lagrangian-Eulerian approach, the computation of the drag force $f_{p_i}$ requires the fluid velocity to be interpolated from the Eulerian frame to the particle location (forward interpolation). In addition, when two-way coupling is accounted for, the force exerted by the particles on the fluid, $f_i^{(p)}$, has to be assessed from the particle data to the Eulerian frame (backward interpolation). Various forward and backward interpolation schemes are proposed in the literature and recently discussed in Garg *et al.* [10]. In the present study, a fourth-order Lagrangian polynomial interpolation is used for the forward interpolation while a linear projection of the particle force over the eight grid nodes surrounding the particle is used for the backward interpolation. These two schemes were shown to be reasonably accurate for a flow with a high spectral content in the fluid velocity field. For the time discretization, the same Runge-Kutta scheme as used for the carrier fluid is used for the particle equation.

The main numerical and flow parameters are provided in table 1 and the particle properties in table 2. Note that the particle diameter is well below the Kolmogorov length scale so that the corresponding particle Reynolds number, $Re_p$, is very small, which justifies the use of the linear Stokes drag law in equation (3). The condition $Re_p \ll 1$ was also checked to be satisfied during the simulation runs. Finally, the ratio of the number of computational particles to the number of real particles is set to one in all the low Reynolds number simulations and does not exceed 3 in the high Reynolds number simulations (up to $2.56 \times 10^8$ particles were tracked).

## 3. Results

Results on the effects of two-way coupling on the settling velocity rate are presented for the Stokes numbers $St = 0.36, 1$ and 2 in decaying homogeneous turbulence at the Reynolds numbers $R_\lambda = 40$ and 130. For this flow configuration identical initial conditions for the fluid (issued from a velocity field of the forced turbulence simulation) and for the particles (random distribution) is used for the three Stokes numbers considered. In the stationary turbulence, the statistics are reported for the Stokes number $St = 1$. They were performed once the average settling velocity exhibited a stationary behavior. The statistical time integrations are given in table 1.

### *3.1. Reynolds number effects: overview*

The average increase of the settling velocity normalized by the terminal velocity, $< \Delta v_s > /v_t =< (v_s - v_t) > /v_t$ (where $v_s$ is the particle settling velocity), is given as a

**Table 3.** Forced turbulence, $R_\lambda = 40$ and 130: average settling rate $< \Delta v_s > /v_t$ and particle Stokes number $St$; $\Phi_v = 3 \times 10^{-5}$, $v_t = v_\eta$.

| | $R_\lambda = 40$ | | $R_\lambda = 130$ | |
|---|---|---|---|---|
| | $St$ | $< \Delta v_s > /v_t$ | $St$ | $< \Delta v_s > /v_t$ |
| 1-way | 1 | 0.479 | 1 | 0.630 |
| 2-way | 1.064 | 0.712 | 1.7 | 0.574 |

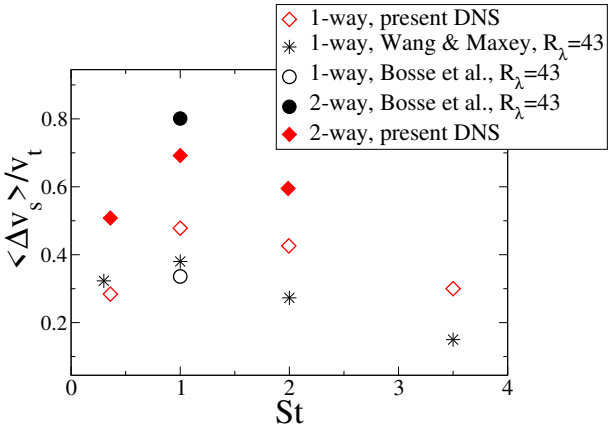


**Figure 1.** Forced turbulence, $R_\lambda = 40$, $v_t = v_\eta (= \eta/t_\eta)$: comparison with previous DNS of the normalized average settling rate $< \Delta v_s > /v_t$ as a function of the Stokes number $St$. For both two-way coupling DNS $\Phi_v = 3 \times 10^{-5}$.

function of the Stokes number $St$ in figure 1 for the one-way and two-way coupling DNS performed for the forced turbulence at $R_\lambda = 40$. In agreement with Wang & Maxey [1] and Bosse *et al.* [5], the present results reproduce the maximum of the settling rate for $St \sim 1$ and also show an additional increase effect by the two-way coupling which is significant for the three Stokes numbers considered. The observed quantitative discrepancies can be mainly attributed to the smaller forcing radius used in the present simulations compared to the one used in the DNS of Wang & Maxey [1] and of Bosse *et al.* [5]. Similar forcing effects were reported by Wang & Maxey [1] for a lower Reynolds number (see figure 7 in [1]). The significant enhancement of the settling velocity by the two-way coupling is also confirmed in the decaying turbulence for identical flow and particle parameters as shown in figure 2(a).

By contrast, the DNS results obtained for $R_\lambda = 130$ show that clear conclusions are difficult to extract regarding the effects of the two-way coupling on the settling velocity. Figure 2(c) exhibits a two-way coupling settling rate well above the corresponding one-way coupling settling rate for $St = 0.36$. However, for the particles with higher inertia, the two-way coupling DNS provide results close to the one-way coupling DNS except at large times where the settling velocity is found larger in the two-way coupling DNS. Regarding the stationary turbulence, the settling rate is found smaller in the two-way coupling simulation (see table 3). Nevertheless, it has to be stressed out that for $R_\lambda = 130$ a direct comparison between two-way and one-way coupling DNS

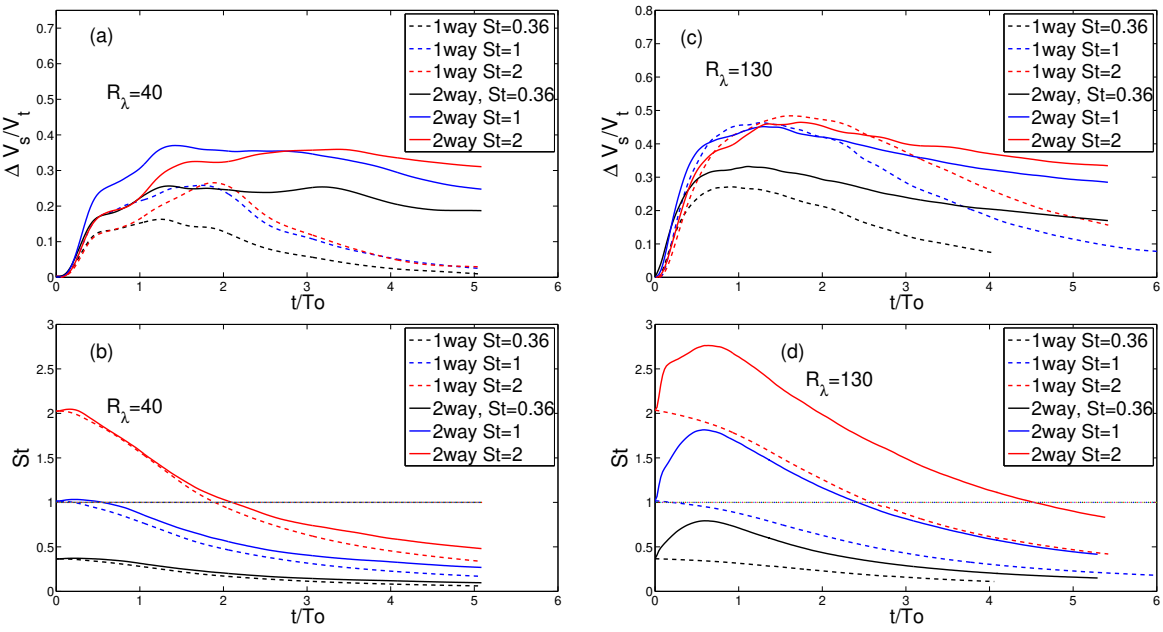


**Figure 2.** Decaying turbulence, $R_\lambda = 40$ and 130: time evolution of the settling rate, $\Delta v_s/v_t$, and of the particle Stokes number, $St$; $\Phi_v = 3 \times 10^{-5}$, $v_t = v_\eta$.

is not consistent because of the large increase of the Stokes number resulting from the interaction of the particles with the fluid. This is shown in figure 2(d) for the decaying turbulence and in table 3 for the stationary turbulence. The enhancement of the particle inertia reflects a significant decrease of the Kolmogorov time scale by the presence of the particles. By comparison, in the low Reynolds number case, figure 2(b) and table 3 show that the Kolmogorov time scale is only slightly reduced by the two-way coupling. Reduction of length flow scales was also observed experimentally by Poelma *et al.* [11] in particle-laden turbulence submitted to gravity effects for different flow and particle parameters from those considered herein. Note that $k_{\max}\eta$ based on the Kolmogorov length scale computed from the two-way coupling simulations takes the minimum instantaneous values 1.04, 1.12 and 1.23 for the respective Stokes numbers $St$=0.36, 1 and 2 in the decaying turbulence case while it takes the value 1.15 for $St = 1$ in the forced turbulence case. These values ensure an adequate numerical resolution.

### *3.2. Turbulence energy redistribution*

Figure 3 compares the instantaneous unladen and laden turbulent flow energy spectra obtained in the decaying turbulence for a given time at which the particle Stokes numbers differ slightly from their initial value. For the low and high Reynolds numbers and for all the Stokes numbers considered, a considerable energy transfer from the particles to the fluid is observed in the large wavenumber range while the low wavenumbers are not significantly modified. In agreement with Yang & Shy [4], the maximum turbulence augmentation at the dissipative scales (very large wavenumbers) is obtained for $St \sim 1$,

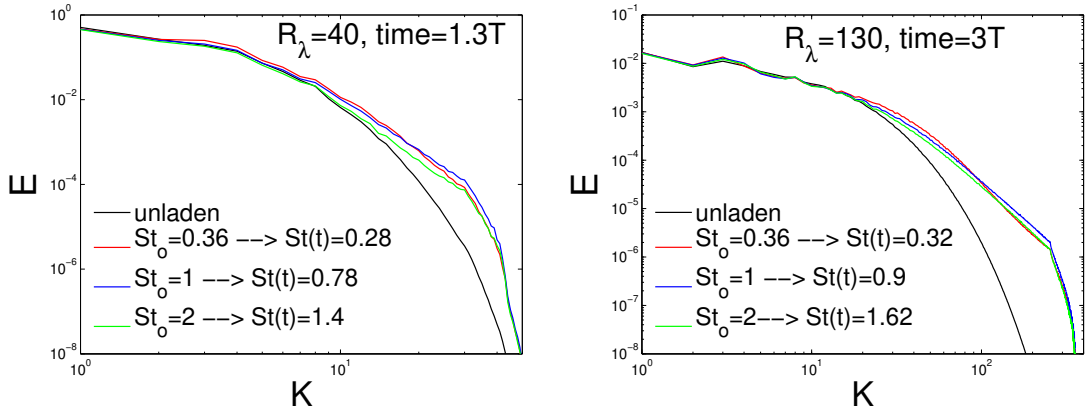


**Figure 3.** Decaying turbulence, $R_\lambda = 40$ and 130: instantaneous three-dimensional energy spectra; $St_o$ refers to the initial Stokes number value and $S(t)$ to the Stokes number value at the considered time. $\Phi_v = 3 \times 10^{-5}$, $v_t = v_\eta$.

at which the preferential concentration is commonly reported to be the most significant. At the intermediate wavenumbers, the turbulence energy spectra present similar features as those found in absence of gravity acceleration by Ferrante & Elghobashi [12].

The redistribution of the turbulence energy is visualized by the energy spectra of the horizontal, $E_{11}$ and $E_{22}$, and vertical, $E_{33}$, components given in figure 4. The spectra show that, under gravity, the turbulence becomes anisotropic with a redistribution of energy from the horizontal to the vertical components. This corroborates the DNS findings of Elghobashi & Truesdel [13], Ferrante & Elghobashi [12] and also the experimental observations of Poelma *et al.* [11]. For the high Reynolds number, the redistribution of energy occurs up to very low wavenumbers while at the low Reynolds number it is damped by viscous dissipation at relatively larger wavenumbers. This may partly explain the significant reduction of the Kolmogorov scales by the particles observed for the high Reynolds number. At the low Reynolds number the energy added by the particles at the small flow scales and redistributed to larger scales is dissipated over the full range of the flow scales as a consequence of the not-complete separation between the energetic and dissipative scales. On the other hand, at the high Reynolds number, dissipation mainly occurs at the small turbulence scales so that the Kolmogorov scales further stretch (and thus decrease) to dissipate part of the additional energy.

The energy spectra obtained in the forced turbulence for $R_\lambda = 40$ and 130 and $St = 1$ (not shown here) exhibit similar features as those reported above for the decaying turbulence.

### *3.3. Particle force field*

An illustration of the preferential concentration effect is supplied by figure 5 which represents the instantaneous particle positions drawn in a transversal plane of the fluid box in the case of the decaying turbulence for the two Reynolds numbers and for $St = 1$. Compared to the low Reynolds number, the particle clusters tend to concentrate in small

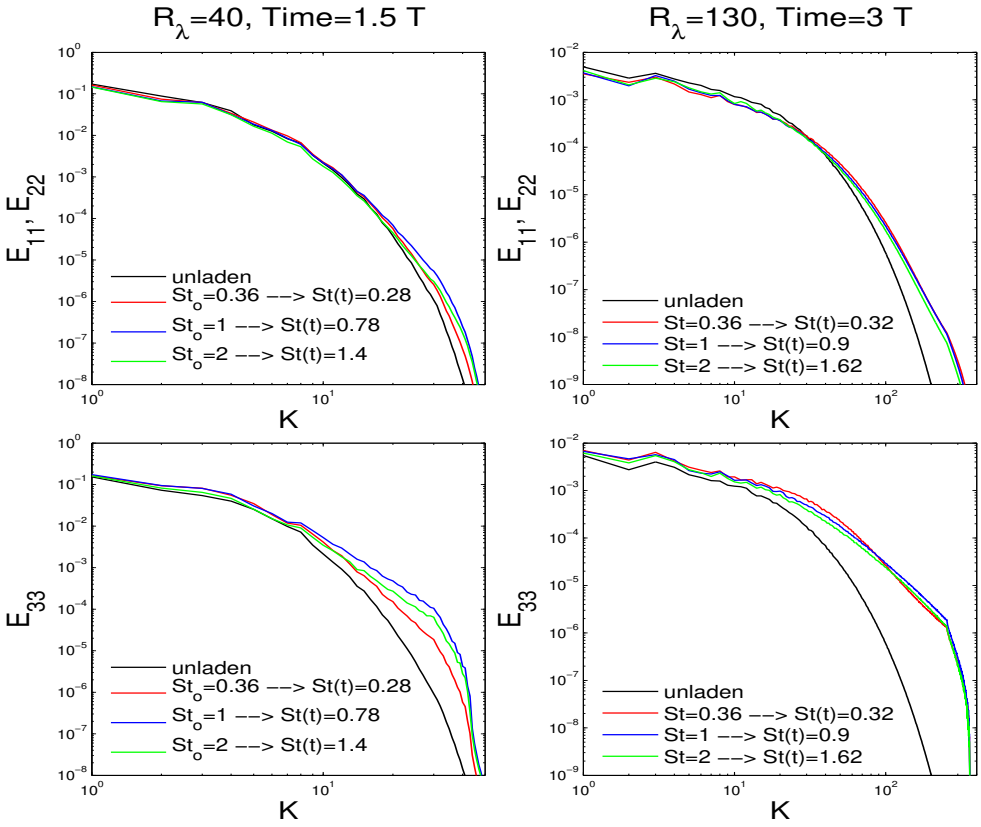


**Figure 4.** Decaying turbulence, $R_\lambda = 40$ and 130: instantaneous vertical and horizontal flow velocity components energy spectra; see legend in figure 3.

flow regions in the high Reynolds number turbulence (see inset for $R_\lambda = 130$). This indicates that particles mainly accumulate at the small turbulence scales, in agreement with the observations of Aliseda *et al.* [3] and Yang & Shy [4]. The force exerted by the particles on the fluid is analyzed in figure 6, by showing the probability density function (PDF) of the particle force density. The large probability for zero force is associated with regions of fluid devoid of particles (see figure 5) and reflects a highly non-homogeneous particle force field due to concentration effects. As shown in figure 6, concentration effects are very small for $St = 0.36$. The particles are shown to mainly exert a negative force on the fluid or equivalently a downward force which in turns accelerates the fluid in the gravity direction. Also, the PDF of large values of the downward force is found to increase when the preferential accumulation of the particles becomes more significant. This is well shown by comparing the PDF obtained for the less inertial particles ($St = 0.36$) with the more inertial ones ($St = 1$ and 2). Note that the downward force exerted by the particles on the fluid must result in an enhancement of the settling velocity. This was clearly observed for $R_\lambda = 40$ but not for $R_\lambda = 130$. The preferential concentration of the particles highly depends on their Stokes number. Thus, for $R_\lambda = 130$, the large

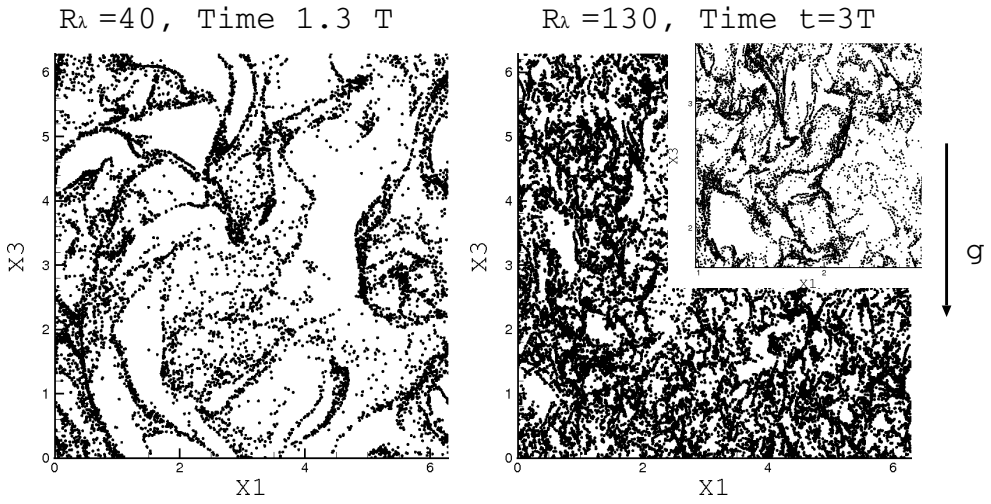


**Figure 5.** Decaying turbulence, $R_\lambda = 40$ and 130: instantaneous particle positions drawn in the plane $X_2 = 2\pi/2$; $\Phi_v = 3 \times 10^{-5}$, $v_t = v_\eta$. The inset for $R_\lambda = 130$ is a inbox zoom of the particle positions field.

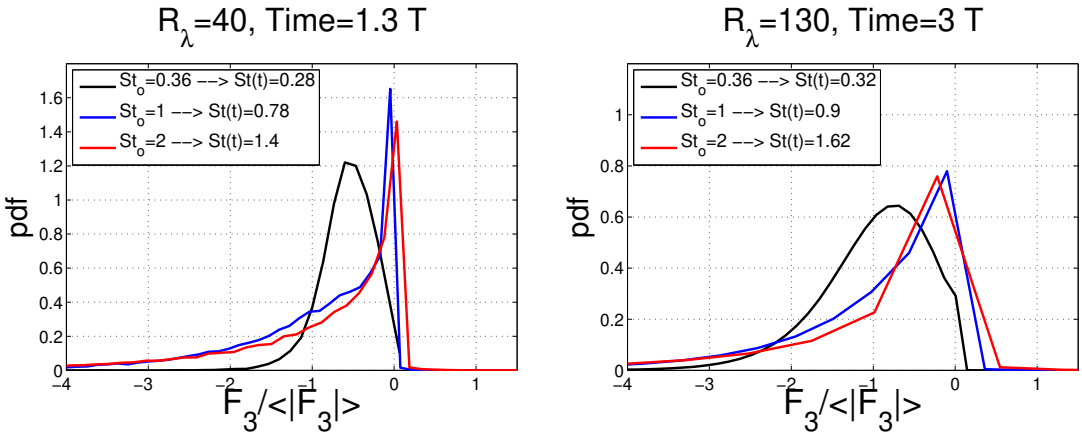


**Figure 6.** Decaying turbulence, $R_\lambda = 40$ and 130: PDF of the force density exerted by the particles on the fluid along the gravity direction; $\Phi_v = 3 \times 10^{-5}$, $v_t = v_\eta$.

increase of $St$ by two-way coupling significantly alters the concentration effects. This in turn implies that the resulting effect of the downward force on the settling velocity is strongly dependent on the modification of the small turbulence scales by the two-way coupling (see comment at the end of next section).

**Table 4.** Forced turbulence, $R_\lambda = 130$: comparison with experiment. $v_t = 0.5u'$ ($v_t = 3.46v_\eta$).

| | DNS, $R_\lambda = 130$ | | | Experiment, $R_\lambda = 120$ |
|---|---|---|---|---|
| | 1-way | 2-way | 2-way | Yang & Shy [4] |
| $\Phi_v \times 10^{-5}$ | - | 1.5 | 3 | 5 |
| $\Phi_m$ | - | 0.075 | 0.15 | $\sim 0.05$ |
| $< \Delta v_s > /v_t$ | 0.216 | 0.326 | 0.366 | 0.24 |
| $< \Delta v_s > /u'$ | 0.106 | 0.153 | 0.165 | 0.13 |
| $u'/u'_o$ | 1 | 1.029 | 1.08 | 1.2 |
| $St$ | 1 | 1.52 | 2.23 | - |

*3.4. Comparison with experiments*

Table 4 compares the present particle and flow DNS data with experimental data given by Yang & Shy [4]. In both the numerical and experimental studies the carrier turbulence is stationary homogeneous and isotropic, the gravity acceleration is such that $v_t = 0.5u'$ and the Stokes number is $St = 1$ (value based on the unladen-flow Kolmogorov time scale). The Reynolds number, volume fraction and mass loading ($\Phi_m = \rho_p \Phi_v / \rho$) are somewhat different in the DNS but still very close to the experimental values. For $\Phi_v = 3 \times 10^{-5}$ the value of $k_{\max}\eta$ is 1.1 so that no higher volume fraction was considered for the sake of numerical resolution.

The average settling rate computed from the one-way and two-way coupling DNS compare reasonably well with the experiment, a better agreement being obtained with the two-way coupling DNS and when the mass loading is closer to the one reported in the experiment. Note that as the volume fraction increases, the settling rate increases as well. This behavior corroborates the experimental observations of Aliseda *et al.* [3]. Table 4 shows that the two-way coupling DNS reproduce the enhancement of the turbulence energy by the particles as observed in the experiments but the ratio of the turbulence intensity of the laden flow to the one of the unladen flow, $u'/u'_o$, is found smaller in the simulations. More important, as previously observed in section 3.1, the DNS show that the particle Stokes number computed *a-posteriori* in the two-way coupling DNS is significantly above its value based on the unladen flow quantities (one-way coupling $St$). This again implies that the Kolmogorov scales have been significantly decreased by the interaction of the particles with the turbulence. This effect can not be experimentally measured as there is no data supplied regarding the modification of the dissipative scales by the particles. The significant alteration of the small flow scales by the presence of the particles found in the present DNS shows that comparisons between one-way coupling simulations and experiments might be not-consistent and that further studies on the modification of the structure of the small turbulence scales by the particles are required.

Note that in section 3.1 (for $v_s = v_\eta$), the two-way coupling effects are shown to result in a net increase of the particle settling velocity for $R_\lambda = 40$ (for all values of $St$ considered) while for $R_\lambda = 130$ they are more ambiguous to interpret. Section 3.3

shows that the resulting force exerted by the particles on the fluid must have an increase effect on the particle settling whatever the Reynolds number considered. Keeping in mind that particle concentration effects are strongly dependent on $St$ (commonly found to be optimum for $St \sim 1$), the significant decrease of the small scales of turbulence (or equivalently the significant increase of $St$) observed in the two-way coupling simulations for the high Reynolds number will in turn alter the particle concentration compared to the one-way coupling simulations. Thus, the enhancement of the particle settling through the downward force may be reduced or increased by a less or more efficient concentration mechanism of the particles depending on the change in $St$. By considering the DNS results reported in table 4, the increase of $St$ (becoming larger than unity) with $\Phi_v$ may suggest a less effective particle concentration as the volume fraction is enhanced and explain that the settling velocity obtained from the one-way and two-way coupling simulations are not drastically different. By contrast, for the low Reynolds number simulations, because of the slight alteration of the dissipative scales by the two-way coupling effects it can be argued that particle concentration effects are similar in the one-way and two-way coupling simulations and that the downward force exerted by the particles on the fluid has a net increase effect on the settling velocity (see table 3). The Reynolds number dependence of two-way coupling effects on the Kolmogorov scales may in part explain the apparent contradiction between the experimental results of Aliseda *et al.* [3] and Yang & Shy [4].

## 4. Conclusions

The present study reported preliminary results from one-way and two-way coupling DNS of heavy particles settling in a low and high Reynolds number homogeneous turbulence. Decaying and stationary turbulence were considered as well as particle inertia effects.

The main results of this study are found similar for both Reynolds numbers in the decaying and forced turbulence simulations. Thus, it can be concluded that the use of a forcing scheme in the simulation of the stationary turbulence does not alter fundamentally the results.

For the low Reynolds number and all the particle Stokes numbers considered, the force exerted by the particles on the fluid has an additional increase effect on the settling velocity when compared to the one-way coupling DNS. This is explained by the alignment of the force with the gravity direction which in turns accelerates the fluid and thus the particles. It is found that the more significant is the preferential concentration of the particles, the larger is the probability of finding large values of this downward force.

For the high Reynolds number, it is shown that the interaction of the particles with the fluid causes a significant decrease of the Kolmogorov time scale. The consequent modification of the Stokes number brings out an important consequence: direct comparison between one-way and two-way coupling DNS is not consistent. The two-way fluid-particle interaction is obviously inherent in experiments so that the consistency of comparisons between one-way coupling DNS and experiments is also questioned. The two-way coupling DNS results are found in fair agreement with the experiment of Yang & Shy [4].

The particle inertia and the small flow scale dynamics play a fundamental role in the

settling of particles in turbulence. In this sense, the present results evidence that the interaction of the particles with the small turbulent vortical structures under gravity must be further investigated in a two-way coupling approach.

**Acknowledgments**

This research was supported by the Ramón y Cajal research program of the Spanish Ministerio de Educación y Ciencia

## References

[1] Wang L P and Maxey M R 1993 *J. Fluid Mech.* **256** 27–68
[2] Yang C Y and Lei U 1998 *J. Fluid Mech.* **371** 179–205
[3] Aliseda A, Cartellier A, Hainaux F and Lasheras J C 2002 *J. Fluid Mech.* **468** 77–105
[4] Yang T S and Shy S S 2005 *J. Fluid Mech.* **526** 171–216
[5] Bosse T, Kleiser L and Meiburg E 2006 *Phys. Fluids* **18** 027102
[6] Maxey M and Riley J 1983 *Phys. Fluids* **26** 883–889
[7] Rogallo R 1981 NASA Techn. Report.
[8] Jímenez J and Wray A A 1998 *J. Fluid Mech.* **373** 255–282
[9] Maxey M R and Patel B K 2001 *Int. J. Multiphase Flow* **27** 1603–1626
[10] Garg R, Narayanan C, Lakehal D and Subramaniam S 2007 *Int. J. Multiphase Flow* **33** 1337–1364
[11] Poelma C, Westerweel J and Ooms G 2007 *J. Fluid Mech.* **589** 315–351
[12] Ferrante A and Elghobashi S 2003 *Phys. Fluids* **15** 315–329
[13] Elghobashi S and Truesdell G C 1993 *Phys. Fluids* **A 5 (7)** 1790–1801